NO reduction with hydrogen over cobalt molybdenum nitride and molybdenum nitride: a comparison study

C. Shi[a,b,c], A.M. Zhu[b], X.F. Yang[b], and C.T. Au[a,*]

[a]*Department of Chemistry, Center for Surface Analysis and Research, Hong Kong Baptist University, Kowloon Tong, Hong Kong*
[b]*Laboratory of Plasma Physical Chemistry, Dalian University of Technology, Dalian 116024, P. R. China*
[c]*Department of Chemistry, Dalian Institute of Light Industry, Dalian 116034, P. R. China*

Received 3 March 2004; accepted 14 May 2004

Cobalt molybdenum nitride (Co_3Mo_3N) and molybdenum nitride (Mo_2N) were investigated for the catalytic reduction of NO with H_2. The latter deactivated rapidly with time on stream, whereas the former remained active and stable over a test period of 30 h. The results of X-ray diffraction (XRD), X-ray photoelectron spectroscopy (XPS), and H_2-temprature-programmed reduction (H_2-TPR) characterization indicated that the deactivation of Mo_2N was due to the bulk oxidation of Mo_2N to MoO_2. As for the Co_3Mo_3N catalyst, despite partial decomposition into Mo_2N and Co, it remained resistant to oxidation. The results suggest that compared to the monometallic nitride, the bimetallic one is more suitable for NO reduction with H_2.

KEY WORDS: cobalt molybdenum nitride; molybdenum nitride; NO reduction.

1. Introduction

It is known that nitrides and carbides of certain transition metals possess excellent catalytic properties in reactions such as CO hydrogenation [1,2], ammonia synthesis [3], hydrotreatment [4–6], isomerization [7,8], freon disposal [9], and automobile exhaust catalysis [10]. Among them, molybdenum nitride has attracted much attention. In reactions such as dehydrogenation, hydrogenolysis, and isomerization, molybdenum nitride was reported to show catalytic behavior resembles that of noble metals [11–13]. The similarity in chemical properties between molybdenum nitrides and noble metals suggests that the former could be effective for the catalytic removal of NO [10,14]. As reported by He *et al.*[10] molybdenum nitride showed high activities for NO direct decomposition: NO conversion to N_2 was ca. 89% at 450 °C, and the conversion remained stable for ca.10 h.

Several bimetallic nitride catalysts have been synthesized and used for ammonia synthesis and hydrogenation reactions [15–20]. Cobalt molybdenum nitrides were prepared by temperature-programmed nitridation of $CoMoO_4$ at 973 K [15–19] or $NH_5(CoOHMoO_4)_2$ at 880 K [20]. It was reported that Co_3Mo_3N was much more active and stable than Mo_2N for ammonia synthesis [15,16]. As for the hydrodenitrogenation of pyridine, the catalytic properties of Co–Mo bimetallic catalyst under medium pressure (3.0 MPa) are much better than those of pure γ-Mo_2N and commercially used sulfided $CoMo/Al_2O_3$ [17]. The promotion effect of Co_3Mo_3N compared to pure γ-Mo_2N has been illustrated in ammonia synthesis and hydrogenation reactions. For the catalytic elimination of NO, only molybdenum nitride was tested. In an attempt of improving the activity and stability of metallic nitrides, we prepared a bimetallic cobalt molybdenum nitride catalyst for NO elimination. In this study, cobalt molybdenum bimetallic nitride catalyst was prepared *via* temperature-programmed nitridation of the corresponding oxides in flowing NH_3, and its catalytic activity and stability for NO reduction with H_2 were compared with those of monometallic molybdenum nitride. Investigations by means of the X-ray diffraction (XRD), X-ray photoelectron spectroscopy (XPS) and H_2-temperature-programmed reduction (H_2-TPR) techniques were carried out for the characterization of the two nitrides.

*To whom correspondence should be addressed.
E-mail: pctau@hkbu.edu.hk

2. Experimental

2.1. Catalyst preparation

Molybdenum trioxide (MoO_3) and cobalt molybdate hydrate ($CoMoO_4 \cdot nH_2O$) were used as precursors for the generation of molybdenum nitride (Mo_2N) and cobalt molybdenum nitride (Co_3Mo_3N), respectively. Cobalt molybdate hydrate ($CoMoO_4 \cdot nH_2O$) was prepared by mixing cobalt nitrate ($Co(NO_3)_2 \cdot 6H_2O$) and ammonium molybdate ($(NH_4)_6Mo_7O_{24} \cdot 4H_2O$) solutions with heating at 80 °C. The blue-purple product was isolated by vacuum filtration and after being rinsed twice with DI water, was dried overnight at 120 °C, and calcined at 500 °C for 3 h.

1011-372X/04/0800–0009/0 © 2004 Plenum Publishing Corporation

The molybdenum nitride catalyst was synthesized by temperature-programmed nitridation of the oxide precursor in flowing ammonia. The procedure was similar to that reported in the literature [10]. Typically, 2.0 g of the oxide precursors was placed in a micro-reactor and a flow of NH_3 (150 mL/min) was introduced into the system. Initially, the sample was linearly heated from room temperature (RT) to 350 °C over a period of 30 min, followed by a rise in temperature from to 450 °C at a rate of 0.5 °C/min, and a further increase from 450 to 700 °C at a rate of 1.25 °C/min. The temperature was then kept at 700 °C for 2 h before cooling to RT in a NH_3 flow. The material was then purged with He for 10 min followed by passivation in 1%O_2 /99% He for 2 h.

2.2. Catalyst Characterization

The surface morphology of the samples was examined using a KYKY 1000 B scanning electron microscope (SEM). Before the experiment, the sample was ground in a mortar and then deposited on a circular copper slide that had been coated with a gold film. The working voltage of the machine is 20 kV and a magnification of 15,000 times was used.

XRD examination was carried out on a X-ray diffractometer (Rigaku D-Max Rotaflex) with CuK_α radiation and Ni filter. XPS measurements were conducted over a spectrometer using Al K_α source operated at 10 kV and 15 mA. Charging effects were corrected by means of adventitious carbon (284.6 eV) referencing.

The temperature-programmed decomposition (TPD) of the nitrides was performed on a flow system equipped with a mass spectrometer (MS, HP G1800A). The sample (100 mg) was first heated from RT to 120 °C in He and maintained at this temperature for 30 min. After being cooled to RT, the sample was directly heated to 950 °C in flowing He at a heating rate of 10 °C/min. The effluent gases were monitored continuously as a function of temperature.

H_2-TPR experiments were carried out in a quartz tube micro-reactor. Before each H_2-TPR run, the sample (20 mg) was heated from RT to 120 °C in Ar and maintained at this temperature for 30 min. After being cooled to RT, the sample was heated from 30 to 950 °C at a rate of 10 °C/min in a mixture of 5%H_2/95%Ar. The effluent gases were monitored by means of a thermal conductivity detector.

Low-temperature O_2 chemisorption capacity was measured by injecting a standard volume of 10% O_2/He via a calibrated loop at 5 min intervals into the catalyst using He as carrier gas until there was no detectable oxygen uptake. Before being admitted, the He and H_2 gases were purified by means of 5A molecular sieve and O_2 purification traps. The adsorption of O_2 was conducted with the catalyst sample being held at −77 °C. Prior to the adsorption, the catalyst was pretreated in H_2 at 400 °C for 2 h, followed by He purging at the same temperature for another 2 h.

2.3. Catalytic activity

The catalytic activity was measured over a micro-catalytic reactor by feeding a gas mixture of 1%H_2/1% NO/98% He to the sample at 400 °C. Typically, the catalyst (0.2 g) was pretreated in pure He at 500 °C for 1 h before the reaction. At a flow rate of 10 mL/min, the corresponding G.H.S.V. was 2400 h^{-1}. The effluent gases were monitored by means of online GC equipped with a thermal conductivity detector. A molecular sieve 5 A column was used to separate H_2, O_2, N_2, and NO. The amount of N_2 produced was used to calculate the conversion of NO to N_2.

3. Results

3.1. Catalyst structure

Figure 1 shows the SEM photographs of Mo_2N and Co_3Mo_3N. It can be seen from the figure that the two nitrides show great differences in morphology. In figure 1A, some larger plate-like shapes and some

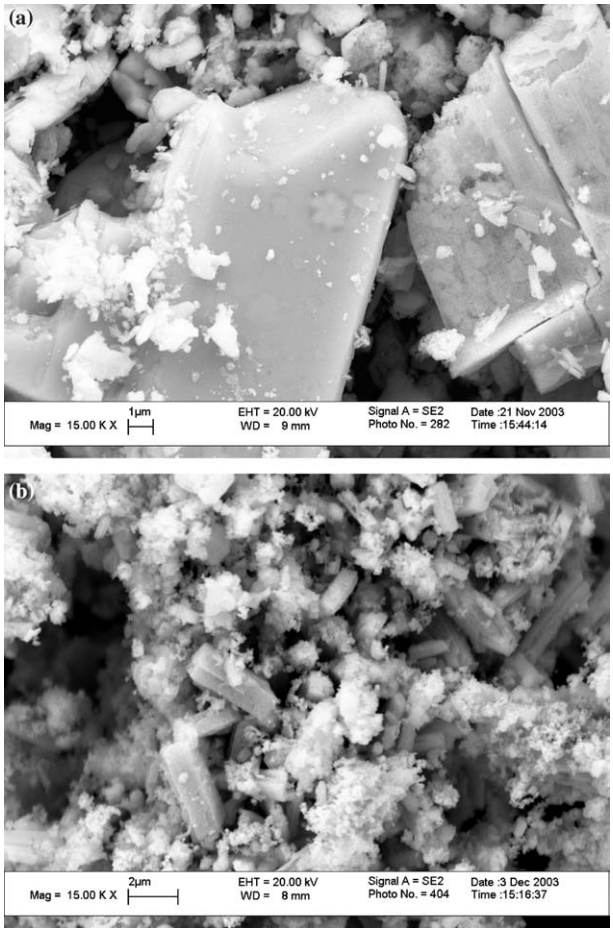

Figure 1. SEM photographs of Mo_2N (a) and Co_3Mo_3N (b).

Table 1
BET surface areas and O_2 chemisorption capacities of Mo_2N and Co_3Mo_3N catalysts at −77 °C

Catalyst	Surface area (m^2/g)	O_2 chemisorption capacity (μmol/g)
Mo_2N	93	68
Co_3Mo_3N	34	26

rod-like aggregates of much smaller, nano-meter sized particles are clearly seen. This is very similar to the Mo_2N morphology reported by Choi *et al.* [21]. As for the bimetallic nitride shown in figure 1B, there is no appearance of larger plate-like shapes, a needle type morphology appears together with rod-like particles. The needle type phase is believed to be attributable to the CoMo phase [22].

List in table 1 are the BET surface areas and O_2 chemisorption capacities of Mo_2N and Co_3Mo_3N. The former shows a larger surface area (93 m^2/g), while that of the latter is relatively small (34 m^2/g); we consider that there is room for optimization of synthesis condition for a higher Co_3Mo_3N surface area [23]. The O_2 chemisorption capacity (at −77 °C) of Mo_2N and Co_3Mo_3N is 68 and 26 μmol/g, respectively; the data compare well with that reported previously [24,25].

The XRD patterns of the as-prepared catalysts are shown in figure 2. The diffraction pattern for Mo_2N shows peaks at 38.2°, 44.2°, 64.0°, and 76.7°, corresponding to {111}, {200}, {220}, and {311} diffractions of bulk γ-Mo_2N. For the as-prepared Co_3Mo_3N sample, peaks are clearly observed at 35.7°, 40.1°, 42.6°, and 46.6°, in good agreement with the Co_3Mo_3N reported by Korlann *et al.* [26].

The oxidation states of molybdenum and distribution of various Mo ions within the as-prepared Mo_2N and Co_3Mo_3N samples were derived from the Mo3d peaks of XPS studies as shown in figure 3. The relative intensities of spin–orbit doublet peaks are given by the ratio of their respective degeneracy, and the $I(3d_{5/2})/I(3d_{3/2})$ intensity ratio for the $Mo3d_{7/2}$–$Mo3d_{5/2}$ doublet is 3/2. A splitting of ~3.13 eV is expected for the doublet. By means of curve-fitting, the distribution of molybdenum oxidation states was estimated. Over Mo_2N, we observed two oxidation states of surface Mo: the peak at binding energy of 232.5 ± 0.2 eV is assigned to the $Mo3d_{5/2}$ component of Mo^{6+}, while that at 229.5 ± 0.2 eV to the

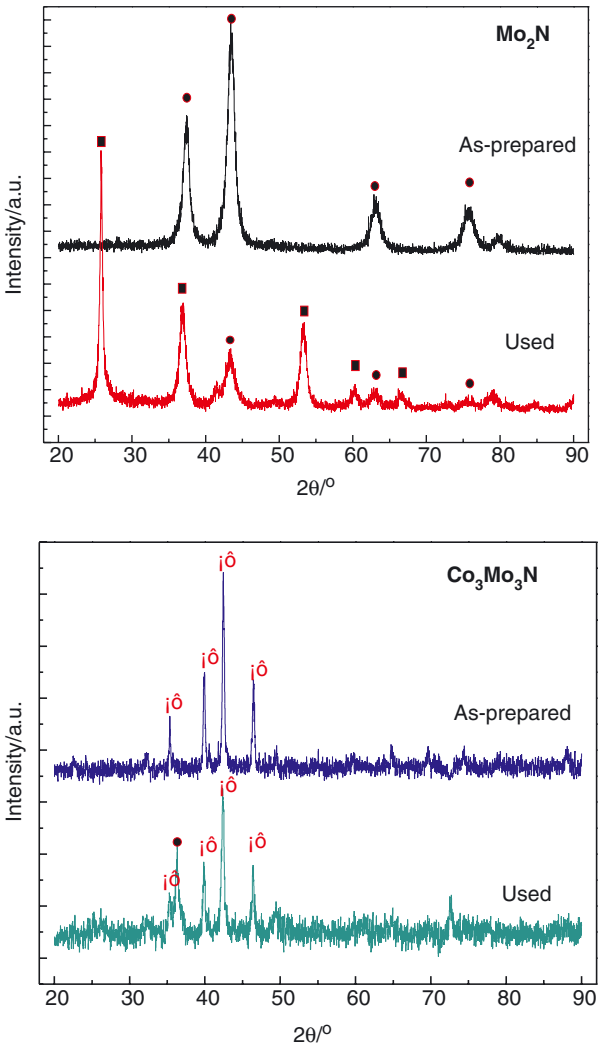

Figure 2. XRD patterns of the as-prepared and used Mo_2N and Co_3Mo_3N catalysts: (●) γ-Mo_2N, (■) MoO_2, (◆) Co_3Mo_3N.

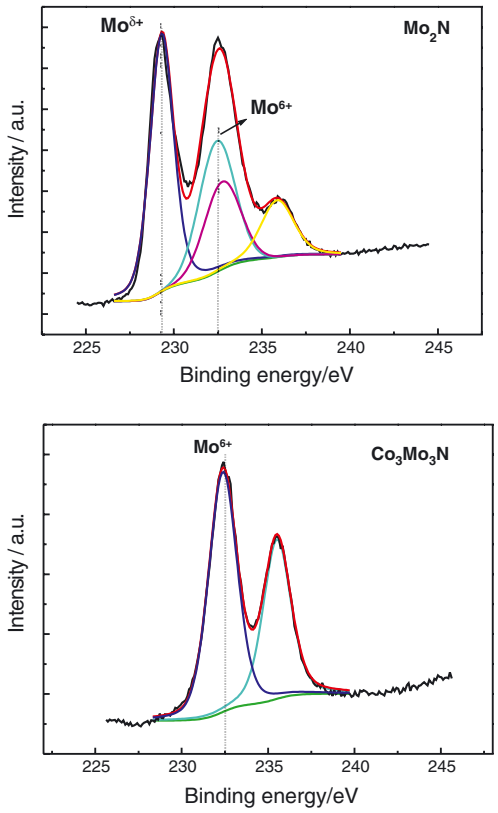

Figure 3. Mo3d XPS spectra of the as-prepared Mo_2N and Co_3Mo_3N catalysts.

$Mo3d_{5/2}$ component of Mo_2N. The 229.5 ± 0.2 eV value is higher than that of Mo^{2+} (228.9 ± 0.2 eV) but slightly lower than that of Mo^{4+} (230.0 ± 0.2 eV). Accordingly, we denote the Mo species of Mo_2N as $Mo^{\delta+}$, where $2 < \delta < 4$. Over Co_3Mo_3N, we observed only one oxidation state at 232.5 ± 0.2 eV due to Mo^{6+}, the highest possible oxidation state of molybdenum.

The TPD profiles of the as-prepared Mo_2N and Co_3Mo_3N samples are presented in figure 4. Over the Mo_2N sample, there are two N_2 peaks at 378 and 510 °C, as well as a more intense one at 890 °C. Over the Co_3Mo_3N sample, N_2 peaks are at much higher temperatures of 520, 720, and 880 °C. There are also desorption peaks of NH_3 and H_2O in the low temperature range from 200 to 400 °C. The MS equipment was not designed for hydrogen detection and the release of H_2 was not monitored. Since the freshly nitrided samples were cooled in a flow of NH_3, it is reasonable to assume that there are NH_x ($x = 1$–3) species on the sample surface as suggested before [27,28]. The NH_3 peak could therefore be considered as the result of desorption of weakly adsorbed NH_3. The broad N_2 desorption band in the range of 500–600 °C should be due to the decomposition of NH_x ($x = 1$–3) species that are strongly adsorbed on the catalyst surface [29]. The N_2 peak at higher temperatures (> 700 °C) can be considered as a result of nitride decomposition [30]; it can be seen that part of the Co_3Mo_3N started to decompose at 720 °C with the release of nitrogen.

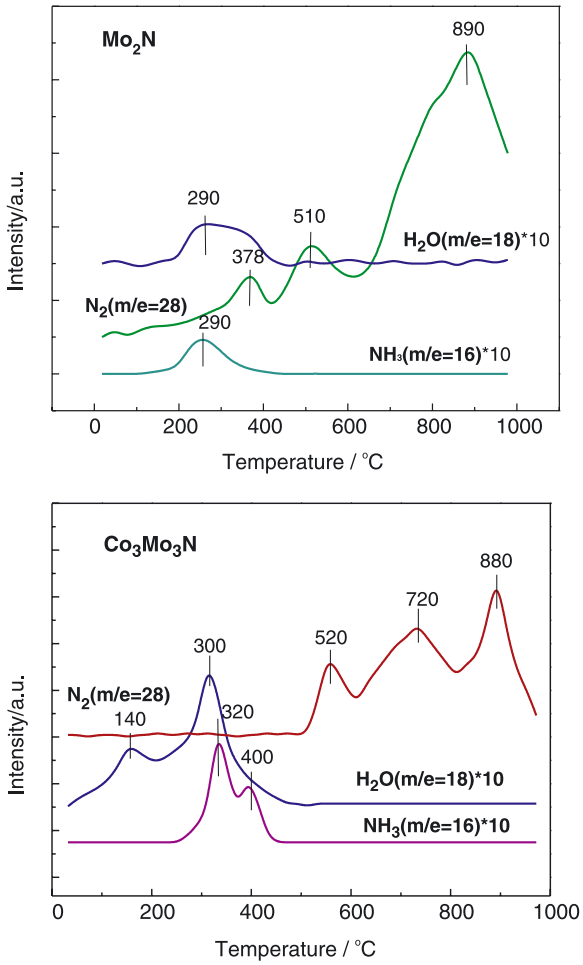

Figure 4. Temperature-programmed decomposition profiles of the as-prepared Mo_2N and Co_3Mo_3N catalysts.

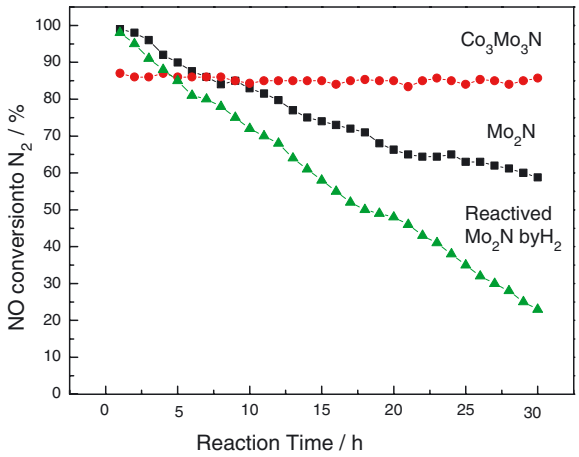

Figure 5. Time dependence of NO conversion to N_2 over the as-prepared Mo_2N, the reactivated Mo_2N (by H_2 reduction), and the as-prepared Co_3Mo_3N catalysts in NO reduction with H_2 at 400 °C.

3.2. Activity measurement

The activity of cobalt molybdenum nitride for NO reduction with H_2 at 400 °C was compared to that of molybdenum nitride (figure 5). The Mo_2N catalyst showed an initial activity of ca. 99% but deactivated with time on stream; NO conversion to N_2 decreased from ca. 99% to ca. 59% within a period of 30 h. The deactivated catalysts can be regenerated by H_2 reduction at 400 °C. However, the regenerated catalyst deactivated quickly in NO/H_2 reaction, as shown in the figure 5. Comparatively, the Co_3Mo_3N catalyst showed much better activity and stability; NO conversion to N_2 stayed at ca. 84% throughout the test period of 30 h.

The activities of the two catalysts for NO reduction with H_2 were reported in term of turnover rates in table 2. The calculation of turnover rates was based on the data of O_2 chemisorption over the Mo_2N and Co_3Mo_3N catalysts. The measurement of O_2 uptakes is an accepted method for estimating the amount of

Table 2
Comparison of turnover rates of Mo_2N and Co_3Mo_3N nitrides for NO reduction with H_2 at 400 °C

Catalyst	Turnover rates after 0.5 h on stream (s^{-1})	Turnover rates after 30 h on stream (s^{-1})
Mo_2N	0.11	0.064
Co_3Mo_3N	0.24	0.24

surface metal atoms of nitrides [26,27]. As indicated by the results of turnover rates, the bimetallic cobalt molybdenum nitride catalyst is considerably more active than the monometallic molybdenum nitride catalyst.

3.3. Characterization of the used catalysts

The X-ray diffraction patterns of the used Mo_2N and Co_3Mo_3N catalysts (functioned in 1%H_2/1%NO/He at 400 °C for 30 h) are also shown in figure 2. Over the used Mo_2N sample, we detected sharp diffraction lines due to MoO_2 ($2\theta = 26.1°$, 36.9°, and 53.2°) crystallites. The γ-Mo_2N lines of the fresh sample could still be identified apart from the MoO_2 features, but in very low intensity. This implies that a large part of the Mo_2N had been oxidized to MoO_2 during the NO reduction reaction. As for the Co_3Mo_3N catalyst functioned in 1%H_2/1%NO/He for 30 h, the diffraction lines of crystallized Co_3Mo_3N remained strong in intensity, and a line at $2\theta = 37.4°$ attributable to γ-Mo_2N diffraction appeared. We detected no lines that could be assigned to metal oxides such as CoO, MoO_3, and $CoMoO_4$.

Summarized in table 3 are the surface atomic concentrations of the as-prepared and used Mo_2N and Co_3Mo_3N catalysts. Compared to the as-prepared Mo_2N sample, the used sample shows an obvious increase in oxygen content, from 40% to 60% after 30 h on stream. The results confirm the accumulation of oxygen on the surface of Mo_2N during NO reduction. Comparing the used Co_3Mo_3N sample with the as-prepared one, one can detect a slight increase in Mo and Co concentration, whereas the concentration of oxygen remains almost unchanged during the reduction reaction.

The H_2-TPR spectra of the fresh and used Mo_2N and Co_3Mo_3N catalysts are shown in figure 6. The H_2-TPR data of MoO_3 and $CoMoO_4$ are also showed for comparison. The spectrum of the as-prepared Mo_2N sample exhibits three major peaks at 360, 680, and 850 °C. Referring to the TPR spectrum of MoO_3, the peaks at 680 and 850 °C should be ascribed to the reduction of MoO_3 to MoO_2 and MoO_2 to Mo, respectively. The peak in the low temperature range (300–500 °C) is due to the reduction of surface NH_x and/or oxygen species. Over the used Mo_2N sample, a strong peak at 725 °C appears. Based on the results of XRD and XPS measurements, it should be due to the reduction of oxygen located in the lattice of molybdenum nitride.

Table 3
Surface atomic concentration of Mo_2N and Co_3Mo_3N catalysts

Element	Atomic concentration (%)			
	Mo_2N		Co_3Mo_3N	
	Fresh	Used	Fresh	Used
Mo3d	48	35	15	17
Co2p	–	–	11	13
N1s	12	5	10	9
O1s	40	60	64	61

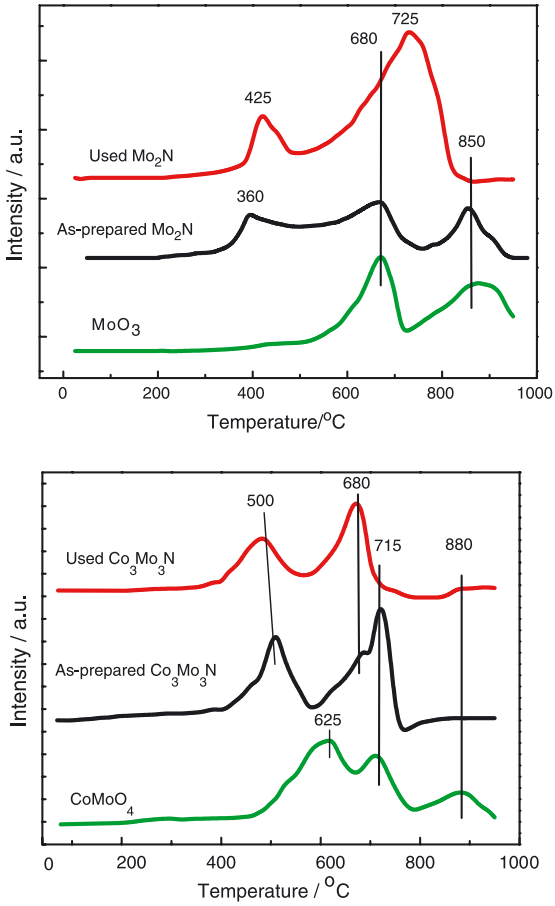

Figure 6. H_2-TPR spectra of as-prepared and used Mo_2N and Co_3Mo_3N catalysts; also added are those of MoO_3 and $CoMoO_4$ for comparison purposes.

As for the as-prepared Co_3Mo_3N sample, the spectrum exhibits two major peaks at 500 and 715 °C with a shoulder at 680 °C, and a broad peak at 880 °C can also be observed. The peak at 500 °C should be due to the reduction of surface NH_x and/or oxygen adspecies. Referring to the H_2-TPR spectra of MoO_3 and $CoMoO_4$, the shoulder at 680 °C should be due to the reduction of MoO_3, and the peak at 715 °C due to the reduction of $CoMoO_4$. Over the used Co_3Mo_3N sample, peaks can be observed at 500, 680 and 880 °C; they can be ascribed to the H_2-reduction of surface NH_x and MoO_3, respectively. However, unlike the case of used Mo_2N, we did not detect any peak possibly due to the reduction of lattice oxygen located in the bulk of Co_3Mo_3N. Moreover, the total area of the H_2-TPR peaks of the as-prepared Co_3Mo_3N sample is similar to that of the used one. In other words, the extent of oxygen incorporation into the Co_3Mo_3N lattice during

the NO reduction reaction was not significant. In the case of Mo_2N, the total area of the H_2-TPR peaks of the used sample is much larger than that of the as-prepared one, suggesting that the extent of oxygen incorporation into the Mo_2N lattice during the NO reduction reaction was much larger. The results are consistent with those of XRD and XPS measurements.

4. Discussion

Transition metal nitrides are important technological materials. They show physical properties that are characteristics of refractory ceramics: very high in melting points, hardness, and tensile strengths. Also, they display electronic and magnetic properties, such as electrical conductivity, Hall coefficient, magnetic susceptibility, and heat capacity resemble those of metals. When applied in catalytic reactions such as ammonia synthesis, Fischer–Tropsch reaction, hydrogenation, oxidation, hydrodenitrogenation and hydrodesulfurization, these materials show activities resemble those of the noble Group 8–10 metals (Pt, Pd, Rh, etc), and in a number of cases, showing superior selectivity, stability, and resistance to poisoning [31,32]. Although there have been only two reports on the application of transition metal nitrides in catalytic NO removal [10,33], the similarity in chemical property between transition metal nitrides and noble metals suggests that the former could be potential catalysts for this reaction.

In an attempt of improving the activity and stability of metallic nitrides, we prepared a bimetallic cobalt molybdenum nitride catalyst for NO elimination. The XRD pattern of Co_3Mo_3N differs greatly from that of Mo_2N, Co_2N, and Co_4N, in good agreement with those reported by Korlann *et al.* [26]. This suggests that the Co_3Mo_3N is a true compound rather than just a physical mixture of monometallic compounds, indicating that the preparation of Co_3Mo_3N is successful.

The catalytic activity and stability of Co_3Mo_3N catalyst for NO reduction with H_2 were compared with those of monometallic molybdenum nitride. In the reduction of NO by H_2, the Mo_2N catalyst showed higher initial activity, but deactivated rapidly with time on stream. Whereas Co_3Mo_3N remained highly active and stable over the tested hours (figure 5).

We adopted techniques of XRD, XPS, and H_2-TPR to characterize the structural changes of nitrides during the NO reduction reaction. In XRD studies, diffraction lines due to molybdenum oxide were observed over the used Mo_2N catalyst, indicating the bulk oxidation of Mo_2N (figure 2). The XPS results showed the accumulation of oxygen on the surface of Mo_2N during the reaction (table 3). The results of H_2-TPR measurement showed a bigger total peak area over the used sample as compared to that of the as-prepared case (figure 6). All the results point to the fact that there was oxygen incorporation into the Mo_2N lattice, and Mo_2N was gradually oxidized during the NO reduction reaction. Accordingly, the deactivation of the Mo_2N catalyst is considered to be a result of Mo_2N oxidation to MoO_2. The deactivated catalysts can be regenerated by H_2 reduction at 400 °C. However, the regenerated catalyst deactivated quickly in NO/H_2 reaction as shown in figure 5. It can be understood that though H_2 reduction can remove oxygen on the surface as well as that in the bulk, the active phase of Mo_2N cannot be restored completely by H_2 reduction. With the regeneration, the percentage of Mo_2N relative to the total Mo species becomes smaller.

As for the used Co_3Mo_3N catalyst, despite its partial decomposition, the catalyst remained active and stable for NO reduction with H_2. After 30 h on stream, there were no XRD diffraction lines due to metal oxides (figure 2). A small portion of Co_3Mo_3N decomposed into Mo_2N and Co after prolonged reaction. It might be due to the small particle size of Co, the Co phase was not detected by wide-angle XRD. The Mo_2N phase that appears in the Co_3Mo_3N sample did not get converted to MoO_2. This might be related to the strong interaction between the Mo_2N and Co phases in the Co_3Mo_3N catalyst, which makes the Mo_2N more resistant to oxidation. The results suggest that the Co_3Mo_3N structure is preserved during the NO reduction reaction, and compared to the Mo_2N catalyst, the Co_3Mo_3N catalyst is more resistant to oxidation. The results of XPS measurements are in consistent with that of XRD measurements: a small portion of Co_3Mo_3N decomposed into γ-Mo_2N and Co after prolonged reaction, causing an increase in Mo and Co concentration on the surface of Co_3Mo_3N. Since Co_3Mo_3N was more oxidation tolerant than Mo_2N, oxygen concentration remained unchanged after prolonged reaction (table 3). Moreover, there were no H_2-reduction peaks possibly due to the reduction of oxygen incorporation into the nitride lattice. The results indicate that Co_3Mo_3N is more resistant to oxidation than Mo_2N.

Then, the question why cobalt molybdenum bimetallic nitride is more resistant to oxidation than monometallic molybdenum nitride arises. One can get insights by looking into the structural differences between Co_3Mo_3N and Mo_2N. It has been suggested that the crystal structure of Co_3Mo_3N is cubic and η-carbide like, with the metal atoms in face-centered cubic (fcc) arrangement and N atoms filling every octahedral interstitial position [34]. The ideal structure consists of eight regular octahedral of Mo atoms centered on a diamond cubic lattice and eight regular tetrahedral of Co atoms centered on a second diamond cubic lattice that interpenetrates the first through a 1/2, 1/2, 1/2 unit cell translation. Sixteen additional Co atoms are coordinated in a tetrahedral fashion around the Co tetrahedral and sixteen N atoms surround the Mo octahedral in tetrahedral coordination as illustrated in figure 7 [35]. A

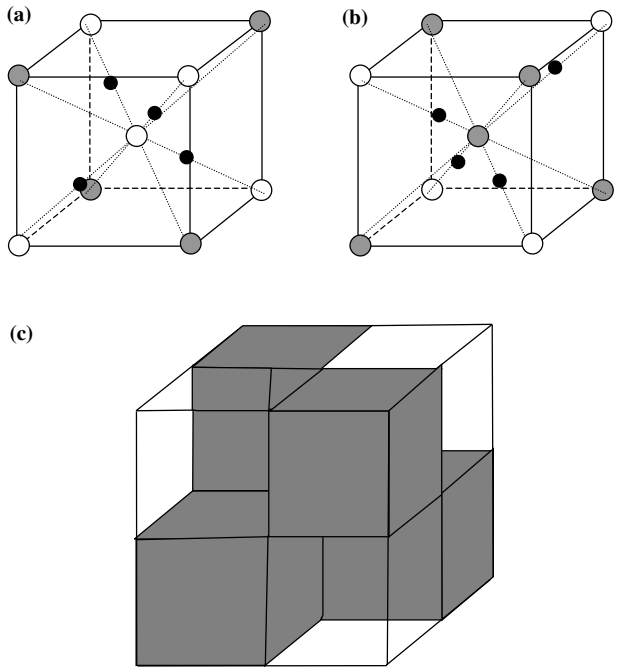

Figure 7. Schematic representation of the Co_3Mo_3N unit cell (after reference [35]). Although Co_3Mo_3N exhibits a large fcc unit cell, its structure can be visualized as composed of two sub-cells, (a) and (b), alternately stacked inside a cubic array (c). In (a) and (b), large white and gray spheres represent Mo and Co atoms, respectively, and the small black spheres interstitial atoms of N. In (c), the sub-cells assume a diamond cubic-type of arrangement in which the Co and Mo atoms are located at the corners and center of the cubic cells.

comparison of the bimetallic compound to the monometallic compound shows considerable differences between the two compounds. Mo_2N exhibits a L'_3 structure with fcc metallic lattice, and N atoms filling only half of the available octahedral vacancies, as illustrated in figure 8 [36]. It is highly likely that the deficiency in such a crystal can be supplemented by oxygen, yielding oxynitride as an intermediate, and finally causing the bulk oxidation of nitrides into oxides.

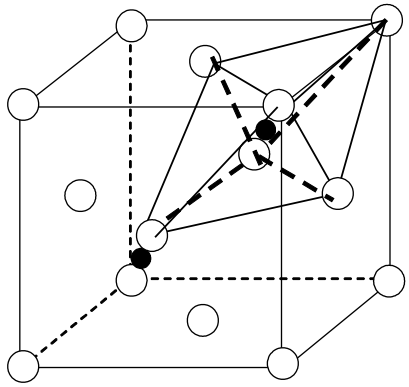

Figure 8. Crystallographic structure of Mo_2N (after reference [36]), where the large white spheres represent Mo atoms and the small black ones represent interstitial atoms of N.

As for Co_3Mo_3N, since there are no unoccupied sites, the incorporation of oxygen into the lattice is not favorable. Actually, the resistance of cobalt bimetallic nitrides to O_2 has been verified before; Yu *et al.* [34] observed identical diffraction patterns and constant lattice parameters after exposing the compound to ambient atmosphere for several months. In addition, as revealed by XPS results (figure 3), all the Mo atoms in Co_3Mo_3N are at the highest possible oxidation state of Mo^{6+}. As for the Mo_2N sample, $Mo^{\delta+}$ ($2 < \delta < 4$) coexists with Mo^{6+}, and further oxidation of molybdenum is possible.

5. Conclusions

Cobalt molybdenum nitride (Co_3Mo_3N) and molybdenum nitride (Mo_2N) catalysts were prepared and tested for the NO reduction with H_2; the former showed much better activity and stability than the latter. The results of XRD, XPS, and H_2-TPR analysis indicated that the deactivation of the Mo_2N catalyst was due to the bulk oxidation of Mo_2N. We observed that the Co_3Mo_3N catalyst is more resistant to oxidation and keeps its structure reasonably well during the reaction.

Acknowledgment

The authors gratefully acknowledge the support of Hong Kong Baptist University (Grant FRG/00-01/II-45) and National Natural Science Foundation of China (No. 20203002).

References

[1] G.S. Ranhotra, A.T. Bell and J.A. Reimer, J. Catal. 108 (1987) 40.
[2] L. Leclercq, K. Imura, S. Yoshida, T. Barbee and M. Boudart, in: *Preparation of Catalysts II*, ed. B. Delmon (Elsevier, Amsterdam, 1978) p. 627.
[3] M. Boudart, S.T. Oyama and L. Leclercq, in: *Proceedings of the. 7th International Conference on Catalysis*, Vol. 1, eds. T. Seiyama and K. Tanabe, (Tokyo, 1980) p. 578.
[4] J.C. Schlatter, S.T. Oyama, J.E. Metcalfe III and J.M. Lambert Jr., Ind. Eng. Chem. Res. 27 (1988) 1648.
[5] E.J. Markel and J.W. Van Zee, J. Catal. 126 (1990) 643.
[6] H. Abe and A.T. Bell, Catal. Lett. 18 (1993) 1.
[7] F.H. Ribeiro, R.A. Dalla Betta, M. Boudart, J. Baumgartner and E. Iglesia, J. Catal. 130 (1991) 86.
[8] F.H. Ribeiro, M. Boudart, R.A.Dalla Betta and E. Iglesia, J. Catal. 130 (1991) 498.
[9] B. Dhanadapani and S.Y. Oyama, Catal. Lett. 35 (1995) 353.
[10] H. He, H.X. Dai, K.Y. Ngan and C.T. Au, Catal. Lett. 71 (2001) 147.
[11] L. Lecercq, M. Provost, H. Pastor, J. Grimblot, A.M. Hardg, L. Gengembre and G. Leclercq, J. Catal. 117 (1989)371.
[12] R.B. Levy and M. Boudart, Science 181 (1973) 547.
[13] J.H. Sinfelt and D.J.C. Yates, Nat. Phys. Sci. 229 (1971) 27.
[14] E. Yasuyuki and K. Hiroshi, Ind. Eng. Chem. Res. 29 (1990) 1583.
[15] R. Kojima and K. Aika, Appl. Catal. A: Gen. 219 (2001) 157.
[16] R. Kojima and K. Aika, Appl. Catal. A: Gen. 215 (2001) 149.

[17] Y. Li, Y. Zhang, R. Raval, C. Li, R. Zhai and Q. Xin, Catal. Lett. 48 (1997) 239.
[18] K. Hada, J. Tanabe, S. Omi and M. Nagai, J. Catal. 207 (2002) 10.
[19] S. Korlann, B. Diaz and M.E. Bussell, Chem. Mater. 14 (2002) 4049.
[20] C.J.H.Jacobsen, Chem. Commun. (2000) 1057.
[21] J. Choi, R.L. Curl and L.T. Thompson, J. Catal. 146 (1994) 218.
[22] D. Kim, D. Lee and S. Ihm, Catal. Lett. 43 (1997) 91.
[23] E.J. Markel and J.W. Van Zee, J. Catal. 126 (1990) 643.
[24] J.W. Jeffrey, J.L. Heiser, K.R. McCrea, B.D. Gates and M.E. Bussell, Catal. Lett. 56 (1998) 165.
[25] K.R. McCrea, J.W. Logan, T.L. Tarbuck, J.L. Heiser and M.E. Bussell, J. Catal. 171 (1997) 255.
[26] S. Korlann, B. Diaz and M.E. Bussel, Chem. Mater. 14 (2002) 4049.
[27] M. Nagai, T. Kusagaya, A. Miyata and S. Omi, Bull. Soc. Chem. Belg. 104 (1995) 311.
[28] C.W. Colling, J.G. Choi and L.T. Thompson, J. Catal. 160 (1996) 35.
[29] M. Nagai, Y. Goto, O. Uchino and S. Omi, Catal. Today 45 (1998) 335.
[30] Z.B. Wei, Q. Xin, P. Grange and B. Delmon, Solid State Ionics, 101 (1997) 761.
[31] S. Ramanathan and S.T. Oyama, J. Phys. Chem. 99 (1995) 16365.
[32] M. Saito and R. B. Anderson, J. Catal. 63 (1980) 438.
[33] E. Yasuyuki and K. Hiroshi, Ind. Eng. Chem. Res. 29 (1990) 1583.
[34] C.C. Yu, S. Ramanathan and S.T. Oyama, J. Catal. 173 (1998) 1.
[35] K. S. Weil and P. N. Kumta, J. Alloy Compd. 265 (1998) 96.
[36] E. Furimsky, Appl. Catal. A: Gen. 240 (2003) 1.